*Biological sciences: Neuroscience*

# Development and aging of cortical thickness correspond to genetic organization patterns

Short title: Genetic organization of cortical development

Anders M Fjell[a,b,1], Håkon Grydeland[a], Stine K Krogsrud[a], Inge Amlien[a], Darius A. Rohani[a], Lia Mork[a], Andreas B Storsve [a], Christian K Tamnes[a], Roser Sala-Llonch[a], Paulina Due-Tønnessen[a,c], Atle Bjørnerud[a,d], Anne Elisabeth Sølsnes[e], Asta K. Håberg[f,g], Jon Skranes[e], Hauke Bartsch[h], Chi-Hua Chen[h], Wesley K Thompson[i], Matthew Panizzon[j], William S Kremen[j,k], Anders M Dale[i,l], Kristine B Walhovd[a,b]

[a] Research Group for Lifespan Changes in Brain and Cognition, Department of Psychology, University of Oslo, 0373, Norway

[b] Department of physical medicine and rehabilitation, Unit of neuropsychology, Oslo University Hospital, 0424, Norway

[c] Department of Radiology, Rikshospitalet, Oslo University Hospital, Norway

[d] The Interventional Centre, Rikshospitalet, Oslo University Hospital, Norway

[e] Department of Laboratory Medicine, Children's and Women's Health, Norwegian University of Science and Technology, Trondheim, Norway

[f] Department of Medical Imaging, St. Olav's Hospital, Trondheim, Norway

[g] Department of Neuroscience, Norwegian University of Science and Technology (NTNU), Trondheim, Norway

[h] Departments of Radiology, University of California, Sa Diego, La Jolla, CA, 92093, USA

[i] Department of Psychiatry, University of California, San Diego, La Jolla

[j] Center of Excellence for Stress and Mental Health, VA San Diego Healthcare System, La Jolla, CA, 92093, USA

[k] Center for Behavioral Genomics Twin Research Laboratory, University of California, San Diego, La Jolla, CA, USA

[l] Department of Neurosciences, University of California, San Diego, La Jolla, CA, 92093, USA

[1] Address correspondence to:

Anders M Fjell, Dept of Psychology, Pb. 1094 Blindern, 0317 Oslo, Norway, Phone: +47 22 84 51 29

Fax: +47 22 84 50 01, e-mail: andersmf@psykologi.uio.no

**Abstract**

There is a growing realization that early life influences have lasting impact on brain function and structure. Recent research has demonstrated that genetic relationships in adults can be used to parcellate the cortex into regions of maximal shared genetic influence, and a major hypothesis is that genetically programmed neurodevelopmental events cause lasting impact on the organization of the cerebral cortex observable decades later. Here we tested how developmental and lifespan changes in cortical thickness fit the underlying genetic organizational principles of cortical thickness in a longitudinal sample of 974 participants between 4.1 and 88.5 years of age with a total of 1633 scans, including 773 scans from children below 12 years. Genetic clustering of cortical thickness was based on an independent dataset of 406 adult twins. Developmental and adult age-related changes in cortical thickness followed closely the genetic organization of the cerebral cortex, with change rates varying as a function of genetic similarity between regions. Cortical regions with overlapping genetic architecture showed correlated developmental and adult age change trajectories, and vice versa for regions with low genetic overlap. Thus, effects of genes on regional variations in cortical thickness in middle age can be traced to regional differences in neurodevelopmental change rates and extrapolated to further adult aging-related cortical thinning. This suggests that genetic factors contribute to cortical changes through life, and calls for a lifespan perspective in research aimed at identifying the genetic and environmental determinants of cortical development and aging.

**Significance statement (120)**

Here we show that developmental and adult aging-related changes in cortical thickness follow closely the genetic organization of the cerebral cortex. 1633 magnetic resonance imaging scans from 974 participants from 4.1 to 88.5 years were used to measure longitudinal changes in cortical thickness, and the topographic pattern of change was compared to the genetic relationship between cortical subdivisions of maximal shared genetic influence, obtained from an independent sample of 406

middle-aged twins. Cortical changes due to maturation and adult age changes adhered to the genetic organization of the cortex, indicating that individual differences in cortical architecture in middle-aged adults have a neurodevelopmental origin, and that genetic factors affect cortical changes through life.

**\body**

There is a growing realization that events during development impact brain and cognition throughout the entire lifespan (1). For instance, the major portion of the relationship between cortical thickness and IQ in old age can be explained by childhood IQ (2), and genotype may explain a substantial part of the life-time stability in intelligence (3). Effects of genes on the organization of the cortex has been shown in adults (4-6), but it is unknown whether and how regional differences in cortical development correspond to these regional genetic subdivisions.

Though consensus is not reached for the exact trajectories, cortical thickness as measured by magnetic resonance imaging (MRI) appears to decrease in childhood (7-12). The exact foundation for this thinning is not known, as MRI provides merely representations of the underlying neurobiology, and available histological data cannot with certainty be used to guide interpretations of MRI results. Although speculative, apparent thickness decrease may be grounded in factors such as synaptic pruning and intracortical myelination, although the link between established synaptic processes (13-15) and cortical thickness has not been empirically confirmed. After childhood, cortical thinning continues throughout the remainder of the lifespan, speculated to reflect neuronal shrinkage and reductions in number of spines and synapses (for a review, see (16)), although similar to development, we lack data to support a direct connection between cortical thinning and specific neurobiological events.

It has been demonstrated that genetic correlations between thickness in different surface locations can be used to parcellate the adult cortex into regions of maximal shared genetic influence (4). This can be interpreted according to the hypothesis that genetically programmed neurodevelopmental events cause lasting impact on the organization of the cerebral cortex detectable decades later (4-6). Here we tested how developmental and lifespan changes fit the genetic organization of cortical

thickness in a large longitudinal sample with 1633 scans from 974 participants between 4.1 and 88.5 years of age, including 773 scans from children below 12 years. Genetically-based subdivisions of cortical thickness from an independent dataset of 406 twins (4) were applied to the data, yielding 12 separate regions under maximum control of shared genetic influences. We hypothesized that thickness in cortical regions with overlapping genetic architecture would show similar developmental and adult age change trajectories, and dissimilar trajectories for regions with low genetic overlap.

**Results**

Across the full age-range of 4.1 to 88.5 years, taking advantage of all longitudinal and cross-sectional observations, generalized additive mixed models (GAMM) were used to fit mean thickness in each hemisphere to age, revealing a high rate of decrease for the first 20 years of life, followed by a more or less steady rate of thinning ($p < .001$ for the smooth effect of age) (Figure 1). A linear function yielded a much poorer fit, as evidenced by increases in Akaike's Information Criterion (AIC) and Bayesian IC (BIC) > 10. Sex did not contribute significantly to the model, and was therefore not included in further analyses.

[*Insert Figure 1 about here*]

The sample was then divided into three age groups: <20years, (1021 scans of 644 participants, mean age at baseline 9.18 years), 20-50 years (234 scans, 136 participants, mean age 35.16 years), and >50 years (378 scans of 194 participants, mean age 64.75 years). Within each group, all available scans were used and a linear mixed effect model (LME) (17) fitted to the data, revealing highly significant thinning over time in each group, controlled for multiple comparisons (Figure 2). A smoothing spline approach was used to estimate annual percent change (APC) in thickness (Figure 3), which exceeded -1.0% for the youngest participants, while APC during the remainder of the life-span typically was between -0.1 and -0.5 depending on region.

[*Insert Figure 2 and Figure 3 about here*]

GAMM was then used to fit thickness to age in each of the 12 genetically defined cortical clusters (Figure 4). All clusters showed monotonic thickness reductions throughout the age-span. To test the extent to which regional variations in longitudinal changes in cortical thickness in development and adulthood resembled the genetic architecture of regional cortical thickness, the mean APC in thickness was calculated for each cluster for the children (< 20 years) and the adults ($\geq$ 20 years) separately, and correlated across all clusters with mean APC across all clusters regressed out. Correlations maps for cortical thickness development and adult age changes were highly similar to the genetic correlations between clusters, i.e. reflecting the genetic relationships among them. The Mantel test confirmed that the relationships between the genetic correlation matrix and the developmental change matrix (observed $r^2 = .80$, $p < 10e^{-5}$) and the adult age change matrix (observed $r^2 = .82$, $p < 10e^{-5}$) were indeed highly significant. The Louvain algorithm for detecting communities in networks was applied to further investigate the similarities between the correlation matrices. The algorithm finds the optimal community structure in each correlation matrix separately. Four identical regions were identified in for development and genetic organization. The first four clusters, motor/pre-motor/SMA, superior and inferior parietal and perisylvian cortex, were grouped together in a superior structure around the central sulcus, the occipital and the ventromedial clusters were grouped together in a posterior structure, and the dorsolateral and medial prefrontal cortex in a frontal structure. Interestingly, ventral frontal cortex was grouped together with the three temporal clusters. For adult changes, the Louvain algorithm suggested a slightly different organization (see SI). Inspection of the correlation matrices revealed that also in adulthood and aging, all the same clusters were correlated, indicating that were no qualitative differences between development, adult age changes and genetic organization with regard to the structure of the correlation matrix. One possible exception was that, in contrast to development and genetic

organization, ventral frontal cortex did not correlate with medial temporal cortex in adults. We also ran the adult analyses restricted to those participants above 50 years to obtain a more typical aging sample, and found that the resulting matrix was very similar to the one obtained with the full adult sample ($r^2$ = .99, p < p < $10e^{-5}$, see SI). The analyses were also run without mean APC regressed out, again yielding correlation matrices highly similar to the genetic clustering (p's < $10e^{-5}$).

[*Insert Figure 3 about here*]

**Discussion**

We found monotonic thinning of the cerebral cortex from 4.1 years throughout the lifespan up to 88.5 years. Neurodevelopmental and adult aging-related changes in cortical thickness followed closely the genetic organization of the cortex, with change rates varying as a function of genetic similarity. This indicates early impact of genes on brain development and age-related changes later in life. The findings are discussed in detail below.

*Cortical thinning throughout the lifespan*

We observed thinning across the entire cortex throughout the age-range from 4.1 to 88.5 years. This is in contrast to earlier findings of regional developmental increases through pre-school and early school years prior to later thinning (10-12, 18-22). However, the results are in line with other recent studies, suggesting monotonic cortical thinning from an early age (7-9, 23-28), and also in agreement with recently published studies of infants observing that cortical thickness in many regions may peak before one or at least two years of age (29, 30). The present findings may indicate that individual differences in offset and/or rate of thinning would be more relevant measures of cortical development than timing of peak cortical thickness. Several recent studies have found thinner cortex to be predictive of favorable cognitive development in school-age years in a variety of cognitive domains (31-37), as well as in neurodevelopmental conditions such as schizophrenia (28, 38).

However, it is important to note that also positive associations between cognitive function and cortical thickness have been found in childhood and adolescence (39, 40), and that symptoms of neurodevelopmental conditions and risk factors have been associated with thinner cortex as well (41-44), even in age-varying ways (45, 46), see Vuoksimaa et al. for a more in-depth discussion on the relationship between cortical thickness and general cognitive abilities (47). These different effects may be due to offset differences between groups and/ or differences in change rates, and indicate a complex relationship between symptoms and cortical developmental markers (48, 49) that likely depends on the condition in question, cortical region and age.

The underlying neurobiological mechanisms of developmental changes in apparent cortical thickness are complex, and involve processes that could lead to early postnatal thickness increase, such as proliferation of dendrites, dendritic spines, axonal sprouting and vascular development, and also processes that would lead to apparent thinning, such as synaptic pruning and intracortical myelination (13-15, 50, 51). The latter could move the boundary detected in MRI between the gray and the white matter outwards to the brain surface, thereby causing apparent thinning of the MRI-reconstructed cortex.

With increasing age, other processes come into play causing further thinning (16). While neuronal number is likely not reduced at any age presently studied, reductions in the number of synaptic spines and synapses may be ongoing in older age at a level where functional consequences are not positive, and shrinkage of cell bodies is another candidate factor underlying cortical thinning in aging (52-54). We have previously reported a mixture of overlapping and spatially distinct patterns of change in maturation and older age (55), and identified a structural brain network sensitive to both (56). Importantly, however, the cognitive correlates of cortical changes are often different in development and aging, as cortical thickness has been more positively associated with cognitive function in older age (57-60). The impact on cognitive function of the observed cortical thinning

seems at least partly different across aging and development, suggesting that either different neurobiological processes are at play, or that the same processes have different consequences in opposite ends of the lifespan. Despite these likely partially differing mechanisms, we see that the regional variations in cortical thinning in development and adulthood correspond to patterns that vary as a function of shared genetic influence.

*Regional differences in cortical development and aging correspond to genetic influences on cortical thickness*

As seen in Figure 4, developmental and aging-related cortical thickness change varied as a function of shared genetic influence, so that genetically close clusters showed more similar rates of maturation and adult changes. The clusters were based on genetic correlations, and represent shared genetic influences on cortical structure between different points on the surface (4). Although some regions corresponded to more traditionally defined anatomical regions based e.g. on cytoarchitectural information or cortical gyrification, the genetic divisions were not identical to traditional regions defined on the basis of structure or function, implying that there is additional information to be obtained by this alternative parcellation of the cortex (4). For the main part, clusters anatomically close to each other are genetically closely related and change in coordinated ways during development and aging. However, not all anatomically close clusters showed converging development and adult change trajectories. For instance, the inferior and superior parietal clusters showed little such convergence with the occipital clusters despite close anatomical localization, and the same was true for the medial and the ventral frontal cortex. Furthermore, there were also instances of clusters involving anatomically more diverse regions that were genetically closely related and showing converging neurodevelopmental and aging relationships. This was true for the ventral frontal cortex and the anterior (“temporal pole”) temporal cluster. These regions showed high genetic correlations with each other, and correlated change rates both in development and adulthood. Although having a common border, the clusters covered anatomically widespread areas.

Direct connections from the ventro-lateral prefrontal cortex to the temporal cortex exist (61, 62), possibly yielding a structural substrate for the observed relationship. This observation has interesting implications, because contrary to genetic covariance of importance for local arealization, effects of genetic variance on regional differences in cortical thickness have been argued to partly correspond to functional specializations rather that anatomical localization only (4). Applying this reasoning to the current results implies that functionally related regions could show more similar structural cortical developmental and adult age change trajectories than functionally less related regions, as has been observed for cortico-subcortical functionally related regions (63).

There were also exceptions to the observed relationship between genetic similarity and synchrony of developmental and adult age-related cortical changes. Change rate in ventromedial occipital cortex during development correlated with middle temporal cortex, while being genetically less related. Thus, although a clear pattern of convergence was seen, correlated developmental or aging-related change did not necessitate genetic convergence.

Importantly, the subdivision of the cortex based on maximal independent genetic influence was performed in a completely independent, cross-sectional sample of middle-aged adult twins (4), but still revealed the same cortical organization that was found to characterize the current developmental and adult age-related cortical changes. This possible genetic influence on neurodevelopmental and adult age trajectories implies either that the effects of genes through early development have life-long impact on cortical thickness, or that the influence of these genes is continuous through life and thereby can be detected at widely different ages. It can be questioned whether a sample of middle-aged males is representative for a mixed-sex developmental sample. We believe that the high degree of overlap between the correlation matrices for development versus the genetic sample indicates that the genetic impact on the adult cerebral cortex (4-6, 64) partly has a neurodevelopmental origin, and that the genetic organization of the cerebral cortex based on the

VETSA sample likely is valid for the developmental and adult samples in the present study. This adheres to a lifespan view on neurocognitive changes, where continuous influences of both genetic make-up and early events can be seen through life. For example, APOE, an important risk factor for sporadic Alzheimer's disease (AD), has been shown to affect brain structure in neonates (65), and variants of the Fat mass and Obesity associated (FTO) gene, being associated with smaller brain volume (66) and increased AD-risk (67) in aging, have been related to smaller brain volumes in adolescence (68).

*Conclusion*

Here we showed continuous thinning of the cerebral cortex from 4.1 to 88.5 years, with both developmental and adult age-related changes in cortical thickness following closely cortical subdivisions based on common genetic influence. This suggests that genetic factors contribute to cortical changes through life, and calls for a lifespan perspective in research aimed at identifying the genetic and environmental determinants of cortical development and aging.

**Materials and Methods**

*Sample*

A total of 1633 valid scans from 974 healthy participants (508 females/ 466 males), 4.1 to 88.5 years of age (mean visit age 25.8, SD 24.1), were drawn from three Norwegian studies coordinated by the Research Group for Lifespan Changes in Brain and Cognition (LCBC), Department of Psychology, University of Oslo, Norway (The Norwegian Mother and Child Cohort Neurocognitive Study (MoBa-Neurocog)/ Neurocognitive Development (ND)/ Cognition and Plasticity Through the Lifespan (CPLS)). For 635 participants, one follow-up scan was available while 24 of these had two follow-ups. Mean follow-up interval was 2.30 years (0.15-6.63 years, SD 1.19). 472 participants were from MoBa-Neurocog (508 girls/ 466 boys, 773 observations, mean age at testing 7.3 years [4.1-12.0], 301 with two tests, mean follow-up interval 1.5 years [1.0-2.2]), and 502 were from ND/CPLS (277 girls, 225

boys, 860 observations, mean age at testing 42.4 years [8.2-88.5], 334 with two tests and 24 with three tests, mean follow-up interval 3.1 years [0.2-6.6]). Sample density was higher in childhood/ adolescence than adulthood, since we expected more rapid changes during that age period (731 observations < 10 years, 275 observations ≥ 10 and < 20 years, 165 observations ≥20 and < 40 years, 213 observations ≥ 40 and < 60 years, and 249 observations 60-88.5 years). The studies were approved by a Norwegian Regional Committee for Medical and Health Research Ethics. The twin sample consisted of 406 men, including 110 monozygotic and 93 dizygotic twin pairs, 51 to 59 years of age (mean age 55.8, SD 2.6). Written informed consent was obtained from all participants older than 12 years of age and from a parent/guardian of volunteers under 16 years of age. Oral informed consent was obtained from all participants under 12 years of age. See SI for details on samples.

*MRI data acquisition and analysis*

Imaging data were acquired using a 12-channel head coil on a 1.5-Tesla Siemens Avanto scanner (Siemens Medical Solutions, Erlangen, Germany) at Oslo University Hospital Rikshospitalet and St. Olav's University Hospital in Trondheim, yielding 2 repeated 3D T1-weighted magnetization prepared rapid gradient echo (MPRAGE): TR/TE/TI = 2400 ms/ 3.61 ms/ 1000 ms, FA = 8°, acquisition matrix 192 × 192, FOV = 192, 160 sagittal slices with voxel sizes 1.25 × 1.25 × 1.2 mm. For most children 4-9 years old, iPAT was used, acquiring multiple T1 scans within a short scan time.

MRI data were processed and analyzed with the longitudinal stream (69, 70) in FreeSurfer 5.3 (http://surfer.nmr.mgh.harvard.edu/) (71, 72). For the children, the issue of movement is especially important, as it could potentially induce bias in the analyses (73). All scans were manually rated for movement on a 1-4 scale, and only scans rated 1 and 2 (no visible or only very minor possible signs of movement) were included. For details on MRI analyses, see SI.

After surface reconstruction, the cortex was parcellated in 12 separate genetic clusters of cortical thickness, each under maximal control of shared genetic influences. This was based on fuzzy cluster analyses of apparent cortical thickness in an independent sample of 406 twins from the Vietnam Era Twin Study of Aging (VETSA) (74). In brief, cluster analyses were used to identify the boundaries of cortical divisions that were maximally genetically correlated, i.e., under control of shared genetic influences on cortical thickness. The procedures are described in detail elsewhere (4).

*Statistical analyses*

First, GAMM implemented in R (www.r-project.org) using the package "mgcv" (75) was used to derive age-functions for mean thickness in each hemisphere based on all 1633 longitudinal and cross-sectional observations, run through the PING data portal (76). Akaike Information Criterion (AIC) (77) and the Bayesian Information Criterion (BIC) was used to guide model selection and help guard against over-fitting. Next, thickness change was tested in thee age-groups by LME implemented in FreeSurfer (17). Multiple comparisons were controlled by a false discovery rate threshold of .05. A nonparametric local smoothing model implemented in Matlab (78) was used to estimate annual percent change (APC) across the brain surface. APC in each genetic cluster was then correlated, separately for the child (age < 20 years) and adult (age $\geq$ 20 years) age span, with mean change across all clusters regressed out. This was compared to the correlation map of the genetic correlations between each of the 12 clusters by use of the Mantel test (79), as implemented in R using the *ade4* package. The community structure or modules in each matrix were obtained using the Louvain algorithm (80), part of the Brain Connectivity Toolbox (http://www.brain-connectivity-toolbox.net) (81).

**Acknowledgement**

This work was supported by the Department of Psychology, University of Oslo (to K.B.W., A.M.F.), the Norwegian Research Council (to K.B.W., A.M.F.) and the project has received funding from the European Research Council's Starting Grant scheme under grant agreements 283634 (to AMF) and 313440 (to KBW). VETSA is supported by U.S. National Institute on Aging grants R01s AG022381, AG018386, and AG018384.

**References**


1. Walhovd KB, Tamnes CK, & Fjell AM (2014) Brain structural maturation and the foundations of cognitive behavioral development. *Current opin neurol* 27(2):176-184.
2. Karama S*, et al.* (2014) Childhood cognitive ability accounts for associations between cognitive ability and brain cortical thickness in old age. *Mol psychiatr* 19(5):555-559.
3. Deary IJ*, et al.* (2012) Genetic contributions to stability and change in intelligence from childhood to old age. *Nature* 482(7384):212-215.
4. Chen CH*, et al.* (2013) Genetic topography of brain morphology. *Proc Natl Acad Sci USA* 110(42):17089-17094.
5. Chen CH*, et al.* (2012) Hierarchical genetic organization of human cortical surface area. *Science* 335(6076):1634-1636.
6. Chen CH*, et al.* (2011) Genetic influences on cortical regionalization in the human brain. *Neuron* 72(4):537-544.
7. Brown TT*, et al.* (2012) Neuroanatomical assessment of biological maturity. *Current biology* 22(18):1693-1698.
8. Amlien IK*, et al.* (2014) Organizing Principles of Human Cortical Development-Thickness and Area from 4 to 30 Years: Insights from Comparative Primate Neuroanatomy. *Cerebral cortex*.
9. Zielinski BA*, et al.* (2014) Longitudinal changes in cortical thickness in autism and typical development. *Brain* 137(Pt 6):1799-1812.
10. Raznahan A*, et al.* (2011) How does your cortex grow? *J Neurosci* 31(19):7174-7177.
11. Sowell ER*, et al.* (2004) Longitudinal mapping of cortical thickness and brain growth in normal children. *J Neurosci* 24(38):8223-8231.
12. Shaw P*, et al.* (2008) Neurodevelopmental trajectories of the human cerebral cortex. *J Neurosci* 28(14):3586-3594.
13. Huttenlocher PR (1979) Synaptic density in human frontal cortex - developmental changes and effects of aging. *Brain research* 163(2):195-205.
14. Huttenlocher PR, De Courten C, Garey LJ, & Van der Loos H (1982) Synaptic development in human cerebral cortex. *Int j neurol*16-17:144-154.
15. Huttenlocher PR & Dabholkar AS (1997) Regional differences in synaptogenesis in human cerebral cortex. *J comp neurol*387(2):167-178.
16. Fjell AM & Wallhovd KB (2010) Structural brain changes in aging: Courses, causes and cognitive consequences. *Reviews in the neurosciences* 21:187-221.
17. Bernal-Rusiel JL*, et al.* (2013) Statistical analysis of longitudinal neuroimage data with Linear Mixed Effects models. *NeuroImage* 66:249-260.
18. Shaw P*, et al.* (2006) Intellectual ability and cortical development in children and adolescents. *Nature* 440(7084):676-679.
19. Shaw P*, et al.* (2007) Attention-deficit/hyperactivity disorder is characterized by a delay in cortical maturation. *Proc Natl Acad Sci USA* 104(49):19649-19654.
20. Raznahan A*, et al.* (2011) Patterns of coordinated anatomical change in human cortical development: a longitudinal neuroimaging study of maturational coupling. *Neuron* 72(5):873-884.
21. Sowell ER*, et al.* (2003) Mapping cortical change across the human life span. *Nat Neurosci* 6(3):309-315.
22. Sowell ER*, et al.* (2007) Sex differences in cortical thickness mapped in 176 healthy individuals between 7 and 87 years of age. *Cerebral cortex* 17(7):1550-1560.
23. Brown TT & Jernigan TL (2012) Brain development during the preschool years. *Neuropsychol rev* 22(4):313-333.
24. Nguyen TV*, et al.* (2013) Testosterone-related cortical maturation across childhood and adolescence. *Cerebral cortex* 23(6):1424-1432.

25. Mutlu AK*, et al.* (2013) Sex differences in thickness, and folding developments throughout the cortex. *NeuroImage* 82:200-207.
26. Mills KL, Lalonde F, Clasen LS, Giedd JN, & Blakemore SJ (2014) Developmental changes in the structure of the social brain in late childhood and adolescence. *Soc cogn aff neurosci*9(1):123-131.
27. Wierenga LM, Langen M, Oranje B, & Durston S (2014) Unique developmental trajectories of cortical thickness and surface area. *NeuroImage* 87:120-126.
28. Gogtay N*, et al.* (2007) Cortical brain development in nonpsychotic siblings of patients with childhood-onset schizophrenia. *Arch gen psychiatr* 64(7):772-780.
29. Li G*, et al.* (2013) Mapping region-specific longitudinal cortical surface expansion from birth to 2 years of age. *Cerebral cortex* 23(11):2724-2733.
30. Lyall AE*, et al.* (2014) Dynamic Development of Regional Cortical Thickness and Surface Area in Early Childhood. *Cerebral cortex*.
31. Squeglia LM, Jacobus J, Sorg SF, Jernigan TL, & Tapert SF (2013) Early adolescent cortical thinning is related to better neuropsychological performance. *Journal of the International Neuropsychological Society : JINS* 19(9):962-970.
32. Tamnes CK*, et al.* (2011) The brain dynamics of intellectual development: waxing and waning white and gray matter. *Neuropsychologia* 49(13):3605-3611.
33. Schnack HG*, et al.* (2014) Changes in Thickness and Surface Area of the Human Cortex and Their Relationship with Intelligence. *Cerebral cortex*.
34. Ostby Y, Tamnes CK, Fjell AM, & Walhovd KB (2011) Morphometry and connectivity of the fronto-parietal verbal working memory network in development. *Neuropsychologia* 49(14):3854-3862.
35. Darki F & Klingberg T (2014) The Role of Fronto-Parietal and Fronto-Striatal Networks in the Development of Working Memory: A Longitudinal Study. *Cerebral cortex*.
36. Ostby Y, Tamnes CK, Fjell AM, & Walhovd KB (2012) Dissociating memory processes in the developing brain: the role of hippocampal volume and cortical thickness in recall after minutes versus days. *Cerebral cortex* 22(2):381-390.
37. Kharitonova M, Martin RE, Gabrieli JD, & Sheridan MA (2013) Cortical gray-matter thinning is associated with age-related improvements on executive function tasks. *Developmental cognitive neuroscience* 6:61-71.
38. Thormodsen R*, et al.* (2013) Age-related cortical thickness differences in adolescents with early-onset schizophrenia compared with healthy adolescents. *Psychiatry research* 214(3):190-196.
39. Karama S*, et al.* (2011) Cortical thickness correlates of specific cognitive performance accounted for by the general factor of intelligence in healthy children aged 6 to 18. *NeuroImage* 55(4):1443-1453.
40. Menary K*, et al.* (2013) Associations between cortical thickness and general intelligence in children, adolescents and young adults. *Intelligence* 41(5):597-606.
41. Ducharme S*, et al.* (2011) Right anterior cingulate cortical thickness and bilateral striatal volume correlate with child behavior checklist aggressive behavior scores in healthy children. *Biol psychiatr*70(3):283-290.
42. Schilling C*, et al.* (2013) Cortical thickness of superior frontal cortex predicts impulsiveness and perceptual reasoning in adolescence. *Mol psychiatr* 18(5):624-630.
43. Shaw P*, et al.* (2006) Longitudinal mapping of cortical thickness and clinical outcome in children and adolescents with attention-deficit/hyperactivity disorder. *Arch gen psychiatr* 63(5):540-549.
44. Walhovd KB*, et al.* (2007) Volumetric cerebral characteristics of children exposed to opiates and other substances in utero. *NeuroImage* 36(4):1331-1344.
45. Walhovd KB, Tamnes CK, Ostby Y, Due-Tonnessen P, & Fjell AM (2012) Normal variation in behavioral adjustment relates to regional differences in cortical thickness in children. *European child & adolescent psychiatry*.

46. Ducharme S*, et al.* (2012) Decreased regional cortical thickness and thinning rate are associated with inattention symptoms in healthy children. *J American Acad Child and Adolescent Psychiatr* 51(1):18-27 e12.
47. Vuoksimaa E*, et al.* (2014) The Genetic Association Between Neocortical Volume and General Cognitive Ability Is Driven by Global Surface Area Rather Than Thickness. *Cerebral cortex*.
48. Bjuland KJ, Lohaugen GC, Martinussen M, & Skranes J (2013) Cortical thickness and cognition in very-low-birth-weight late teenagers. *Early human development* 89(6):371-380.
49. Martinussen M*, et al.* (2005) Cerebral cortex thickness in 15-year-old adolescents with low birth weight measured by an automated MRI-based method. *Brain* 128(Pt 11):2588-2596.
50. Petanjek Z, Judas M, Kostovic I, & Uylings HB (2008) Lifespan alterations of basal dendritic trees of pyramidal neurons in the human prefrontal cortex: a layer-specific pattern. *Cerebral cortex* 18(4):915-929.
51. Petanjek Z*, et al.* (2011) Extraordinary neoteny of synaptic spines in the human prefrontal cortex. *Proc Natl Acad Sci USA* 108(32):13281-13286.
52. Esiri MM (2007) Ageing and the brain. *J pathology* 211(2):181-187.
53. Jacobs B, Driscoll L, & Schall M (1997) Life-span dendritic and spine changes in areas 10 and 18 of human cortex: a quantitative Golgi study. *J comp neurol*386(4):661-680.
54. Freeman SH*, et al.* (2008) Preservation of neuronal number despite age-related cortical brain atrophy in elderly subjects without Alzheimer disease. *J neuropathol exp neurol* 67(12):1205-1212.
55. Tamnes CK*, et al.* (2013) Brain development and aging: overlapping and unique patterns of change. *NeuroImage* 68:63-74.
56. Douaud G*, et al.* (2014) A common brain network links development, aging, and vulnerability to disease. *Proc Natl Acad Sci USA* 111(49):17648-17653.
57. Dickerson BC*, et al.* (2008) Detection of cortical thickness correlates of cognitive performance: Reliability across MRI scan sessions, scanners, and field strengths. *NeuroImage* 39(1):10-18.
58. Engvig A*, et al.* (2010) Effects of memory training on cortical thickness in the elderly. *NeuroImage* 52(4):1667-1676.
59. Walhovd KB*, et al.* (2006) Regional cortical thickness matters in recall after months more than minutes. *NeuroImage* 31(3):1343-1351.
60. Walhovd KB*, et al.* (2010) Multi-modal imaging predicts memory performance in normal aging and cognitive decline. *Neurobiol aging* 31(7):1107-1121.
61. Petrides M & Pandya DN (2002) Comparative cytoarchitectonic analysis of the human and the macaque ventrolateral prefrontal cortex and corticocortical connection patterns in the monkey. *Eur j neurosci* 16(2):291-310.
62. Takahashi E, Ohki K, & Kim DS (2007) Diffusion tensor studies dissociated two fronto-temporal pathways in the human memory system. *NeuroImage* 34(2):827-838.
63. Walhovd KB*, et al.* (2014) Maturation of Cortico-Subcortical Structural Networks--Segregation and Overlap of Medial Temporal and Fronto-Striatal Systems in Development. *Cerebral cortex*.
64. Desrivieres S*, et al.* (2015) Single nucleotide polymorphism in the neuroplastin locus associates with cortical thickness and intellectual ability in adolescents. *Mol psychiatr* 20(2):263-274.
65. Knickmeyer RC*, et al.* (2014) Common variants in psychiatric risk genes predict brain structure at birth. *Cerebral cortex* 24(5):1230-1246.
66. Ho AJ*, et al.* (2010) A commonly carried allele of the obesity-related FTO gene is associated with reduced brain volume in the healthy elderly. *Proc Natl Acad Sci USA* 107(18):8404-8409.
67. Reitz C*, et al.* (2012) Genetic variants in the Fat and Obesity Associated (FTO) gene and risk of Alzheimer's disease. *PloS one* 7(12):e50354.
68. Melka MG*, et al.* (2013) FTO, obesity and the adolescent brain. *Hum mol genet* 22(5):1050-1058.

69. Reuter M & Fischl B (2011) Avoiding asymmetry-induced bias in longitudinal image processing. *NeuroImage* 57(1):19-21.
70. Reuter M, Schmansky NJ, Rosas HD, & Fischl B (2012) Within-subject template estimation for unbiased longitudinal image analysis. *NeuroImage* 61(4):1402-1418.
71. Dale AM, Sereno, M. I. (1993) Improved localization of cortical activity by combining EEG and MEG with MRI cortical surface reconstruction: a linear approach. *J Cogn Neurosci* 5:162-176.
72. Dale AM, Fischl B, & Sereno MI (1999) Cortical surface-based analysis. I. Segmentation and surface reconstruction. *NeuroImage* 9(2):179-194.
73. Reuter M*, et al.* (2015) Head motion during MRI acquisition reduces gray matter volume and thickness estimates. *NeuroImage* 107:107-115.
74. Kremen WS, Franz CE, & Lyons MJ (2013) VETSA: the Vietnam Era Twin Study of Aging. *Twin res hum genet* 16(1):399-402.
75. Wood SN (2006) *Generalized Additive Models:an introduction with R* (Chapman & Hall/CRC Texts in Statistical Science).
76. Bartsch H, Thompson WK, Jernigan TL, & Dale AM (2014) A web-portal for interactive data exploration, visualization, and hypothesis testing. *Front neuroinformatics* 8:25.
77. Akaike H (1974) A new look at the statistical model identification. *IEEE Trans. Automat. Contr* 19:716-723.
78. Fjell AM*, et al.* (2010) When does brain aging accelerate? Dangers of quadratic fits in cross-sectional studies. *NeuroImage* 50(4):1376-1383.
79. Mantel N (1967) The detection of disease clustering and a generalized regression approach. *Cancer research* 27(2):209-220.
80. Blondel VD, Guillaume J-L, Lambiotte R, & Lefebvre E (2008) Fast unfolding of communities in large networks. *J Statistical Mechanics: Theory and Experiment* P10008.
81. Rubinov M & Sporns O (2010) Complex network measures of brain connectivity: uses and interpretations. *NeuroImage* 52(3):1059-1069.
82. Magnus P*, et al.* (2006) Cohort profile: the Norwegian Mother and Child Cohort Study (MoBa). *Int j epidemiol* 35(5):1146-1150.
83. Krogsrud SK*, et al.* (2014) Development of hippocampal subfield volumes from 4 to 22 years. *Hum brain mapp* 35(11):5646-5657.
84. Wechsler D (1999) *Wechsler abbreviated scale of intelligence* (The Psychological Corporation, San Antonio, TX).
85. Wechsler D (1989) *Wechsler Preschool and Primary Scale of Intelligence* (The Psychological Corporation, San Antonio, TX).
86. Westlye LT*, et al.* (2010) Life-span changes of the human brain white matter: diffusion tensor imaging (DTI) and volumetry. *Cerebral cortex* 20(9):2055-2068.
87. Tamnes CK*, et al.* (2010) Brain maturation in adolescence and young adulthood: regional age-related changes in cortical thickness and white matter volume and microstructure. *Cerebral cortex* 20(3):534-548.
88. Beck AT & Steer R (1987) *Beck Depression Inventory Scoring manual* (The Psychological Corporation, New York).
89. Folstein MF, Folstein SE, & McHugh PR (1975) "Mini-mental state". A practical method for grading the cognitive state of patients for the clinician. *J Psychiatr Res* 12(3):189-198.
90. Kremen WS*, et al.* (2006) Genes, environment, and time: the Vietnam Era Twin Study of Aging (VETSA). *Twin res hum genet* 9(6):1009-1022.
91. Panizzon MS*, et al.* (2010) Testosterone modifies the effect of APOE genotype on hippocampal volume in middle-aged men. *Neurology* 75(10):874-880.
92. Panizzon MS*, et al.* (2012) Genetic influences on hippocampal volume differ as a function of testosterone level in middle-aged men. *NeuroImage* 59(2):1123-1131.
93. Kremen WS*, et al.* (2010) Salivary cortisol and prefrontal cortical thickness in middle-aged men: A twin study. *NeuroImage* 53(3):1093-1102.

94. Prom-Wormley E*, et al.* (2015) Genetic and environmental contributions to the relationships between brain structure and average lifetime cigarette use. *Behav Genet* 45(2):157-170.
95. Fennema-Notestine C*, et al.* (2011) Presence of ApoE epsilon4 allele associated with thinner frontal cortex in middle age. *J Alzheimers Dis* 26 Suppl 3:49-60.
96. Kremen WS*, et al.* (2013) Genetics of brain structure: contributions from the Vietnam Era Twin Study of Aging. *Am J Med Genet B Neuropsychiatr Genet* 162B(7):751-761.
97. Wonderlick JS*, et al.* (2009) Reliability of MRI-derived cortical and subcortical morphometric measures: effects of pulse sequence, voxel geometry, and parallel imaging. *NeuroImage* 44(4):1324-1333.
98. Fischl B & Dale AM (2000) Measuring the thickness of the human cerebral cortex from magnetic resonance images. *Proc Natl Acad Sci USA* 97(20):11050-11055.
99. Rosas HD*, et al.* (2002) Regional and progressive thinning of the cortical ribbon in Huntington's disease. *Neurology* 58(5):695-701.
100. Kuperberg GR*, et al.* (2003) Regionally localized thinning of the cerebral cortex in schizophrenia. *Arch Gen Psychiatry* 60(9):878-888.
101. Reuter M, Rosas HD, & Fischl B (2010) Highly accurate inverse consistent registration: a robust approach. *NeuroImage* 53(4):1181-1196.
102. Fischl B, Sereno MI, Tootell RB, & Dale AM (1999) High-resolution intersubject averaging and a coordinate system for the cortical surface. *Hum Brain Mapp* 8(4):272-284.
103. Lin X & Zhang D (1999) Inference in generalized additive moxed models by using smoothing splines. *J Royal Stat Soc, series B* 61:381-400.
104. Team RC (2013) *A language and environment for statistical computing.* (R Foundation for Statistical Computing, Vienna).
105. Fjell AM*, et al.* (2009) Minute effects of sex on the aging brain: a multisample magnetic resonance imaging study of healthy aging and Alzheimer's disease. *J Neurosci* 29(27):8774-8783.

**Figure legends**

**Figure 1 Global change in cortical thickness**

GAMM was used to estimate the lifespan trajectory of cortical thickness separately for each hemisphere, based on both the cross-sectional and the longitudinal information in the 1633 observations in the total sample. The shaded area around the fit line represents 95% confidence interval. Green signifies female and pink signifies male.

**Figure 2 Regional change in cortical thickness**

Thinning of the cerebral cortex as tested LME using all cross-sectional and longitudinal data. Results are thresholded at false discovery rate < .05 to control for familywise errors, thus the left end of the p-value scale will vary slightly between age groups and hemispheres.

**Figure 3 Annual percent thickness decrease across the lifespan**

Annual percent change (APC) in cortical thickness was estimated from a surface-based smoothing spline function, yielding APC estimates at each decade from 4 years. Left hemisphere in the upper panel, right in the lower. Blue-cyan colors indicate thinning.

**Figure 4 Overlap between genetic organization of cortical thickness and developmental and aging-related change**

Panel A: The cortex was parcellated into 12 regions (clusters) of maximal shared genetic influence, based on an independent sample of 406 middle aged twins (4). The fuzzy clusters as shown were thresholded at 0.5.

Panel B: Genetic correlations between the clusters are shown in the middle panel. The genetic correlation matrix was compared to the correlations matrices for representing the relationships between cortical thickness change in the same clusters in development (< 20years, left panel) and

aging (≥ 20 years, right panel). The Louvain algorithm was run to find the optimal community structure in each correlation matrix separately, illustrated by the black lines within the color charts, and the development and genetic clusters were ordered according to this algorithm. For aging, the Louvain algorithm suggested a slightly different organization (SI), and to allow comparisons with the two matrices, the same cluster ordering is used, without the community structure shown.

Panel C: Thickness in each genetically defined cluster was demeaned and fitted to age by use of GAMM, and plotted together with the mean of all clusters for comparison purposes. The width of the fit line represents 95% confidence interval. The y-axes are optimized for the data range for each cluster. The blue lines represent the demeaned trajectory for each cluster, while the red lines represent the mean of all clusters.

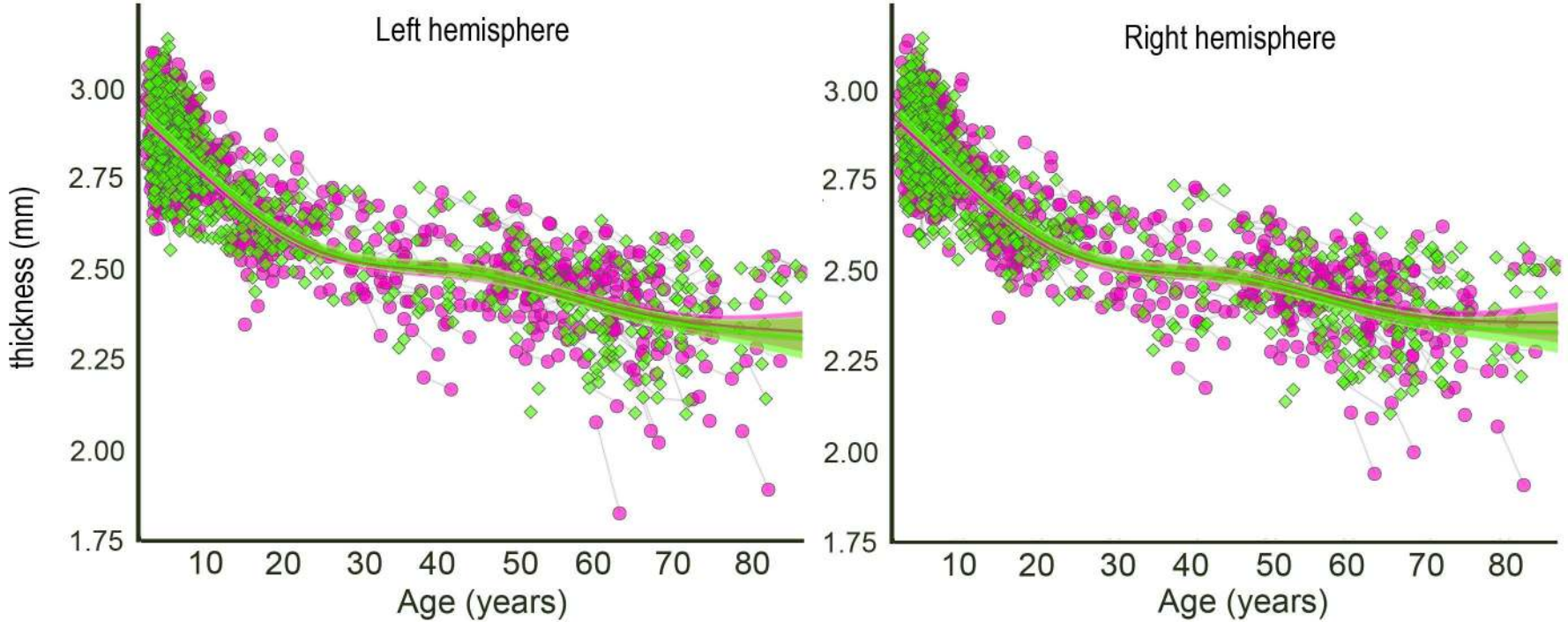
Left hemisphere
Right hemisphere
thickness (mm)
3.00
2.75
2.50
2.25
2.00
1.75
10
20
30
40
50
60
70
80
Age (years)

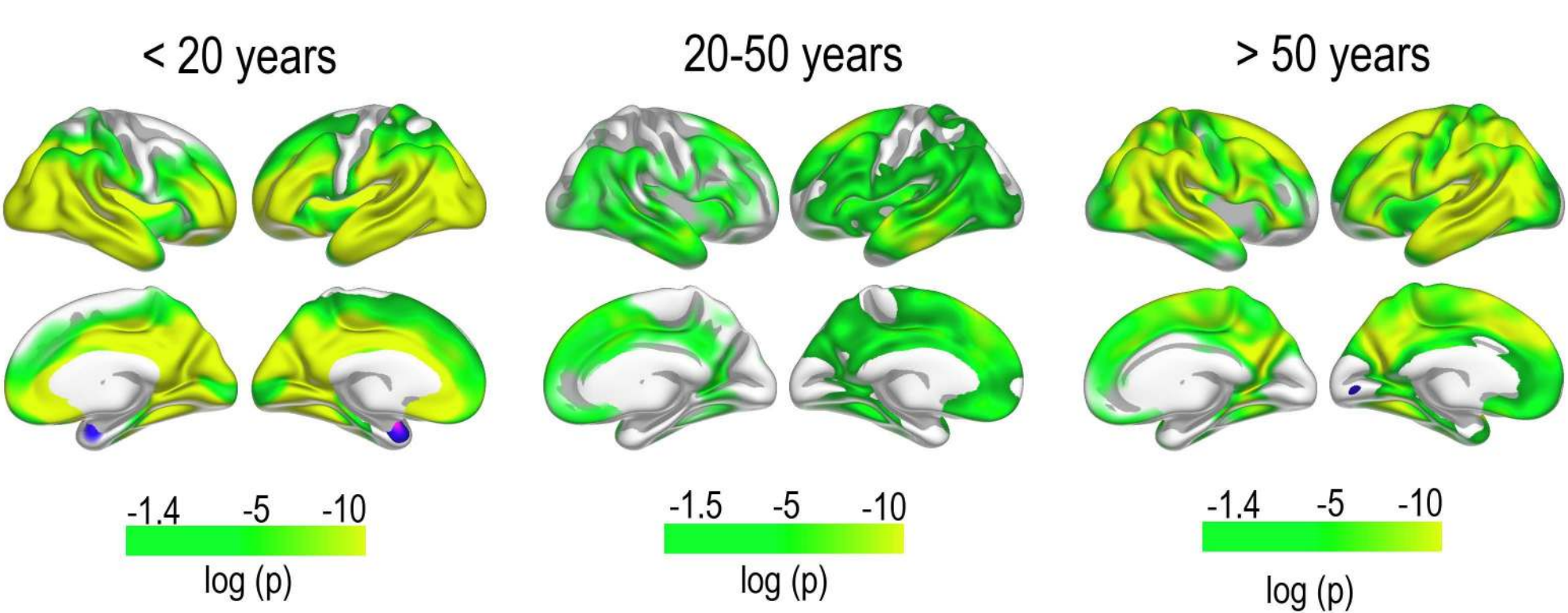
< 20 years
20-50 years
> 50 years
-1.4
-5
-10
log (p)
-1.5
-5
-10
log (p)
-1.4
-5
-10
log (p)

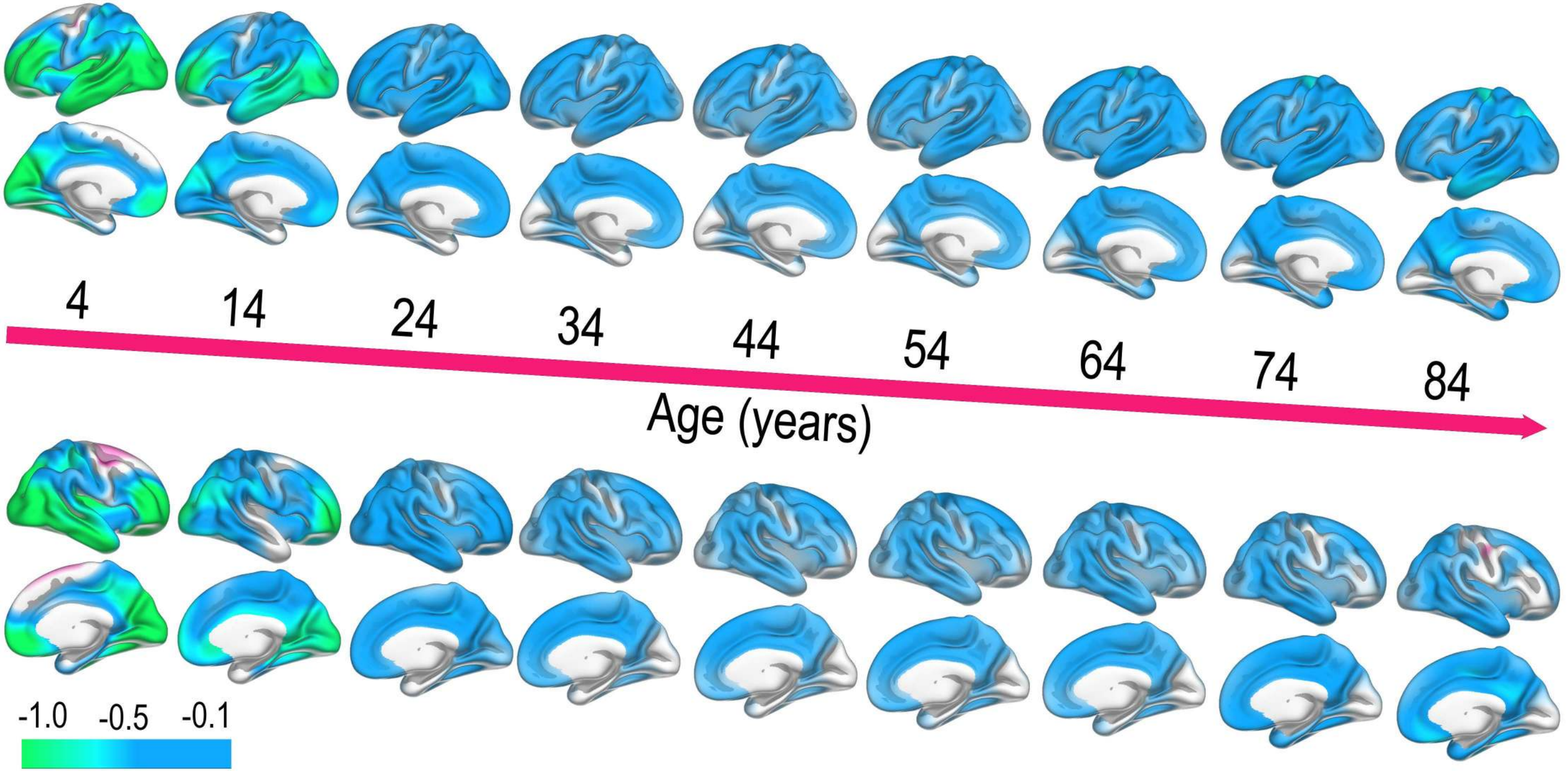
4
14
24
34
44
54
64
74
84
Age (years)
-1.0
-0.5
-0.1
Annual % change

(A)

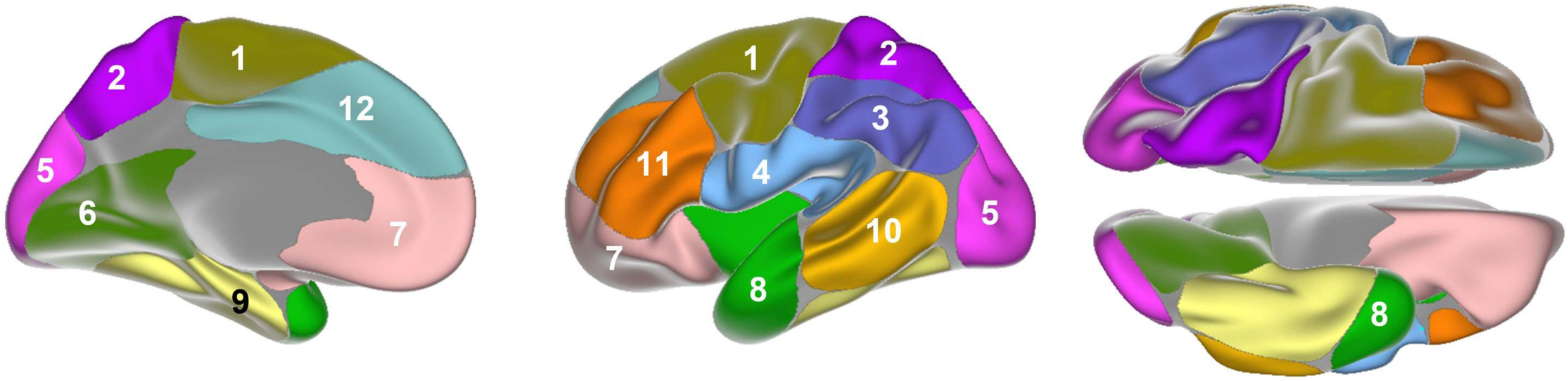
1
2
12
5
6
7
9
1
2
3
11
4
5
10
7
8
8

(B)

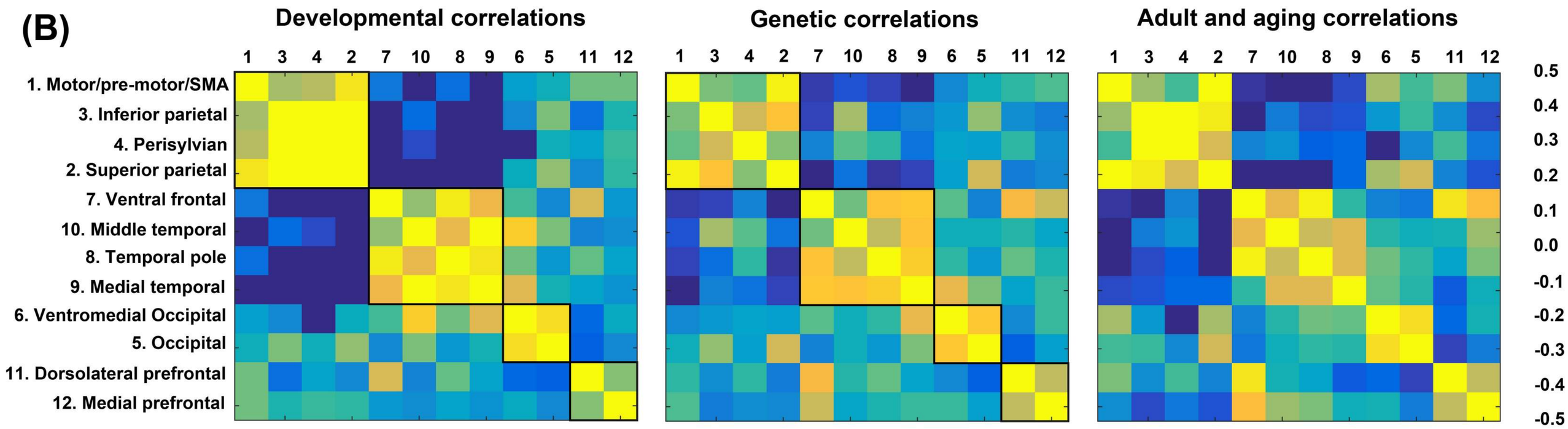
Developmental correlations
Genetic correlations
Adult and aging correlations
1 3 4 2 7 10 8 9 6 5 11 12
1. Motor/pre-motor/SMA
3. Inferior parietal
4. Perisylvian
2. Superior parietal
7. Ventral frontal
10. Middle temporal
8. Temporal pole
9. Medial temporal
6. Ventromedial Occipital
5. Occipital
11. Dorsolateral prefrontal
12. Medial prefrontal
0.5
0.4
0.3
0.2
0.1
0.0
-0.1
-0.2
-0.3
-0.4
-0.5

(C)


Motor/pre-motor/SMA
Superior parietal
Inferior parietal
Perisylvian
Occipital
Ventromedial occipital
Ventral prefrontal
Temporal pole
Medial temporal cortex
Middle temporal
Dorsolateral prefrontal
Medial prefrontal
4 20 40 60 80
Demeaned thickness (mm)
years
Lower
Higher
Relative thickness
cluster
mean

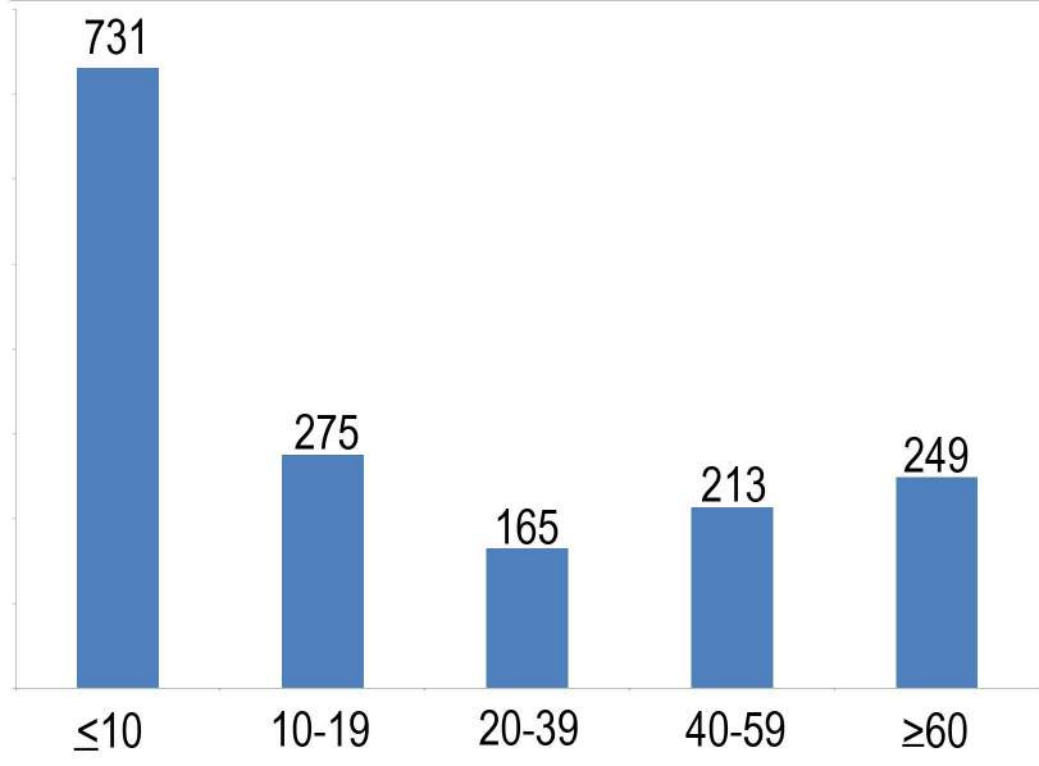
731
275
165
213
249
≤10
10-19
20-39
40-59
≥60

## Left hemisphere thickness

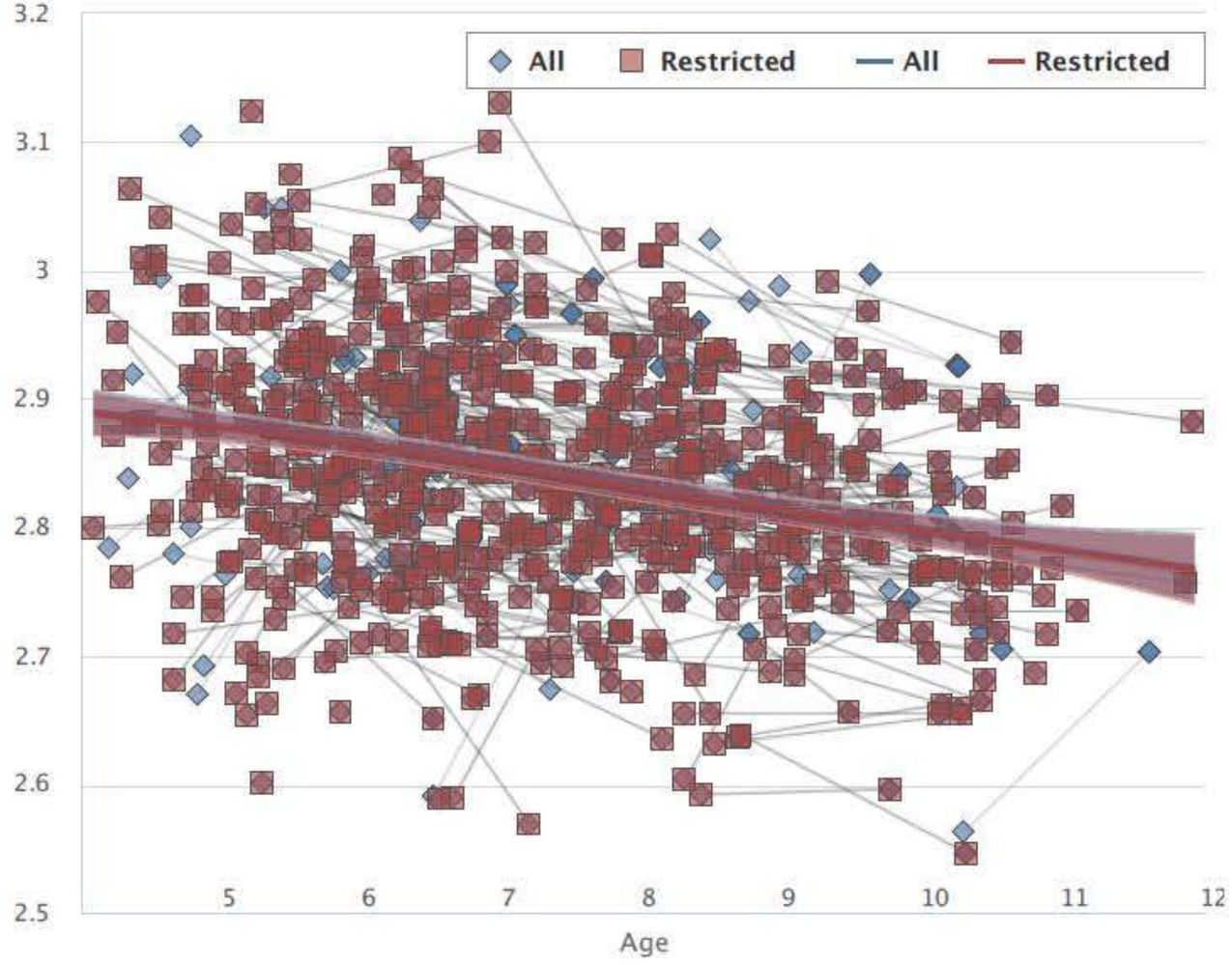


## Right hemisphere thickness

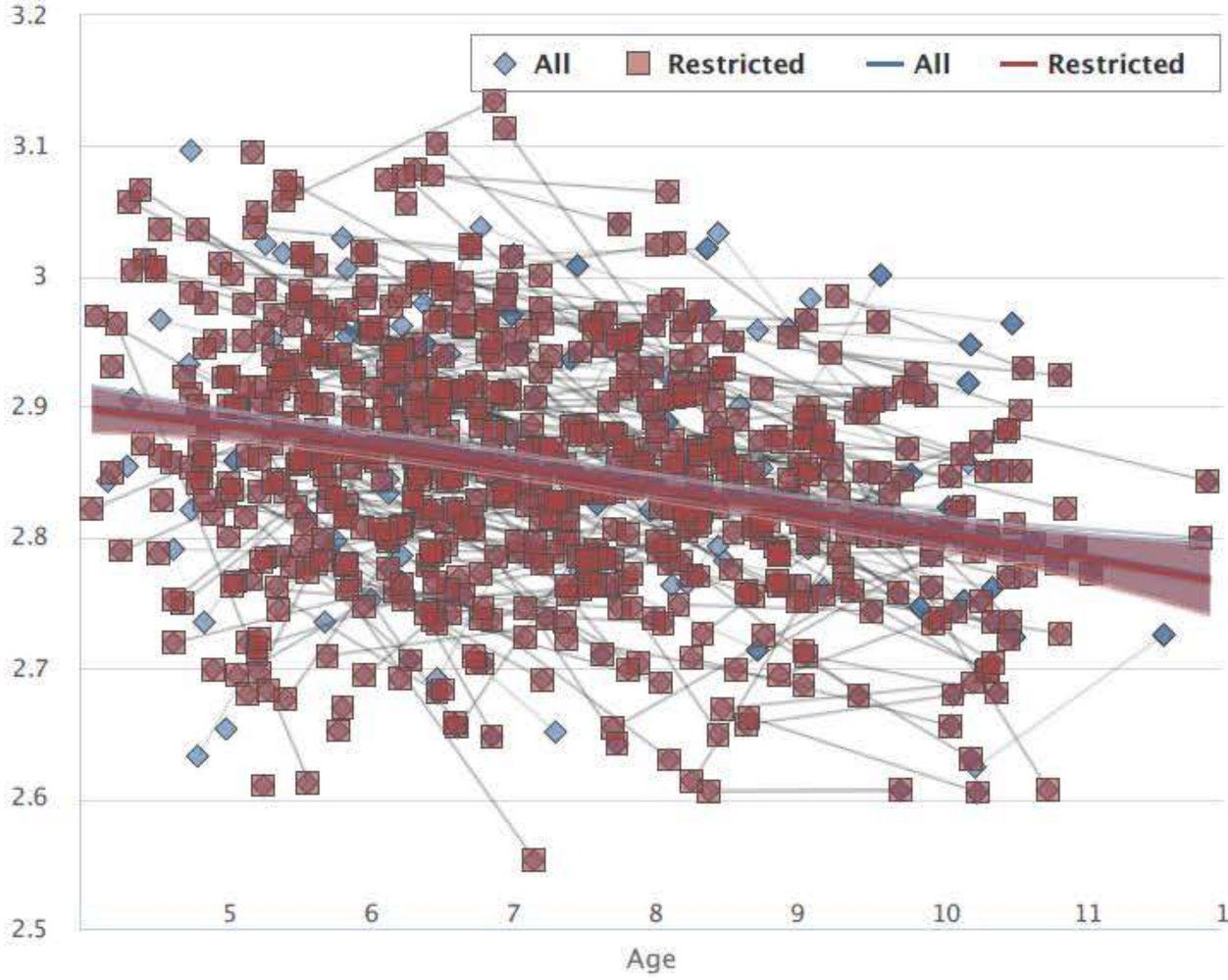

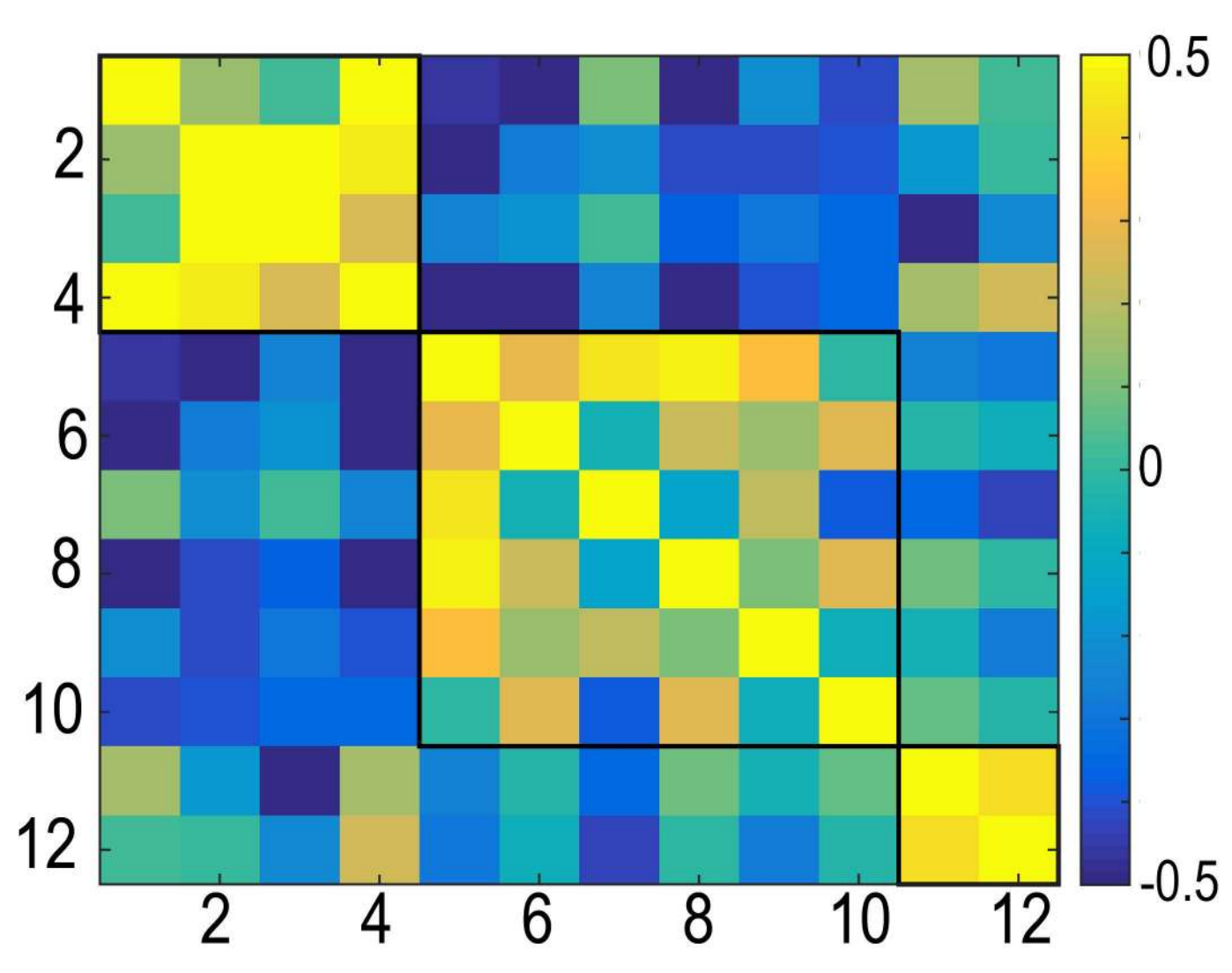
2
4
6
8
10
12
2
4
6
8
10
12
0.5
0
-0.5

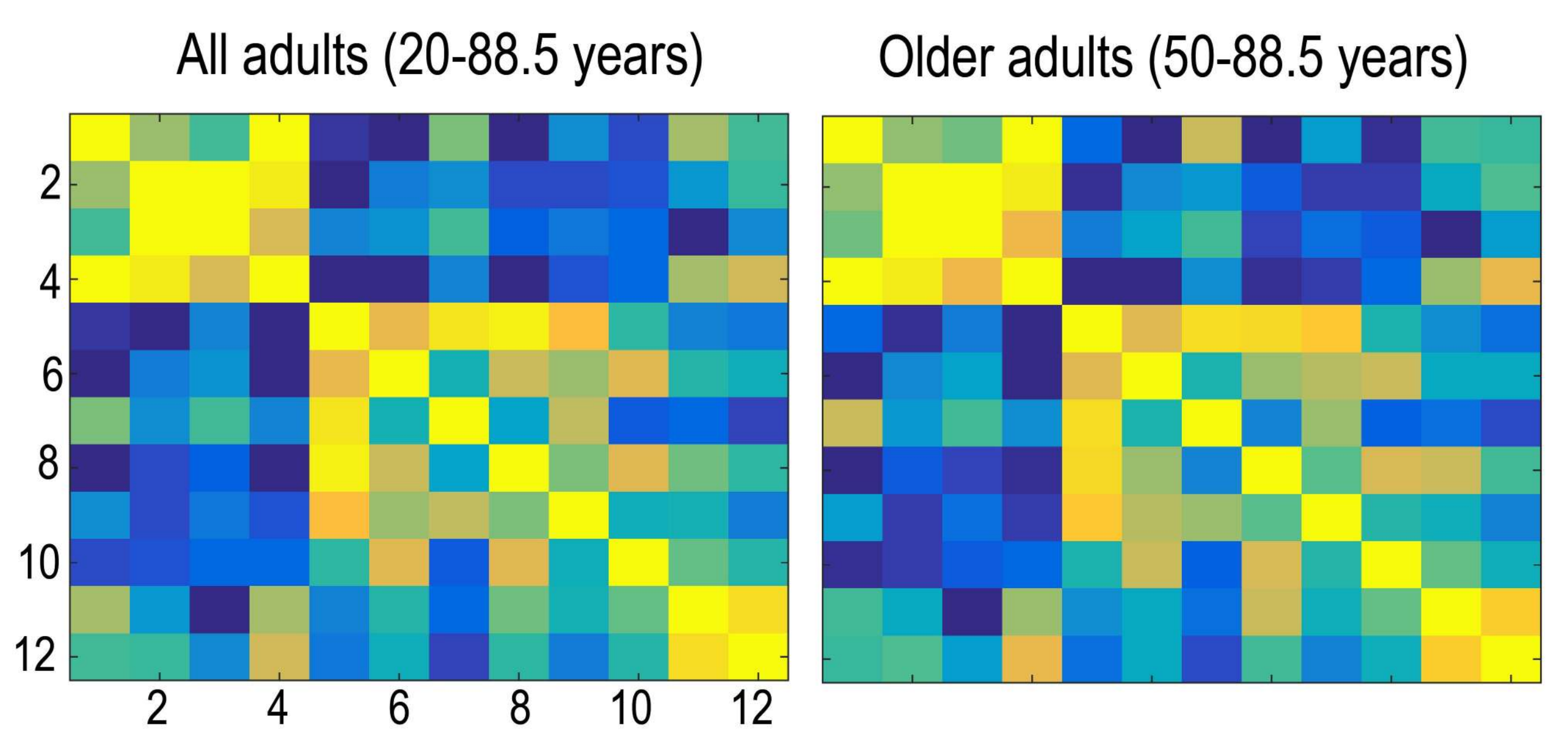
All adults (20-88.5 years)
Older adults (50-88.5 years)
2
4
6
8
10
12
2
4
6
8
10
12

Supplemental Information for

# Development and aging of cortical thickness corresponds to genetic organization patterns

Anders M Fjell[a,b,1], Håkon Grydeland[a], Stine K Krogsrud[a], Inge Amlien[a], Darius A. Rohani[a], Lia Mork[a], Andreas B Storsve [a], Christian K Tamnes[a], Roser Sala-Llonch[a], Paulina Due-Tønnessen[a,c], Atle Bjørnerud[a,d], Anne Elisabeth Sølsnes[e], Asta K. Håberg[f,g], Jon Skranes[e], Hauke Bartsch[h], Chi-Hua Chen[h], Wesley K Thompson[i], Matthew Panizzon[j], William S Kremen[j,k], Anders M Dale[i,l], Kristine B Walhovd[a,b]

**Sample**

All participants' scans were examined by a neuroradiologist, and deemed free of significant injuries or conditions. The studies were approved by a Norwegian Regional Committee for Medical and Health Research Ethics. An overview of sample characteristics is given in Supplemental Table 1 and the distribution of observations across the age range in Supplemental Figure 1.

*[Insert Supplemental Figure 1 and Supplemental Table 1 about here]*

MoBa-Neurocog is a population based sample, with participants were recruited by the Norwegian Medical Birth Registry through the national Norwegian Mother and Child Cohort Study (82), see (8, 83). All participants in the cohort study living in the greater Oslo area or the greater Trondheim area were invited to participate in this study. Valid MRI scans were obtained from 472 participants (age 4.1 to 10.7 years at baseline, 231 girls and 241 boys), and since the project is conceptualized as a population-based community-sample study, all were included in the initial analyses. For 301 participants, valid scans at both baseline and follow up were acquired. Additional analyses were run with very strict criteria for inclusion, including only children with 4500g $\leq$ birth weight $\leq$ 2500g, and general ability level > 1 SD below population mean (Wechsler's Abbreviated Scale of Intelligence or

Wechsler's Preschool and Primary Scale of Intelligence) (84, 85), reducing the MoBa-Neurocog sample to 277 participants with longitudinal MRI for these analyses. 532 of the MoBa-Neurocog scans were performed in Oslo and 241 in Trondheim, on identical scanners with identical scanning parameters and sequences (see below). To ensure that site did not influence the results, a general linear model was run with cluster thickness (12 levels) as repeated measure, site as between subject factor and age as covariate, revealing no significant effect of site on thickness at Tp1 ($F = 1.035$, $p = .31$) or Tp2 ($F = 1.040$, $p = .31$).

Participants from NCD and CPLS were recruited through newspaper advertisements, and local schools and workplaces (n = 502). Detailed criteria for exclusion at baseline are described in (86, 87). The participants were screened using a standardized health interview prior to inclusion in the study. Participants with a history of self- or parent-reported neurological or psychiatric conditions, including clinically significant stroke, serious head injury, untreated hypertension, diabetes, and use of psychoactive drugs within the last two years, were excluded. Further, participants reporting worries concerning their cognitive status, including memory function, were excluded. All participants above 20 years of age scored <16 on Beck Depression Inventory (88) and participants above 40 years of age >26 on Mini Mental State Examination (89). General cognitive abilities were assessed by Wechsler Abbreviated Scale of Intelligence (WASI) (84). All participants scored within normal or high IQ range (82-145).

For some analyses, the sample was split into three age groups. Sample characteristics for each age group are given in Supplemental Table 2.

*[Insert Supplemental Table 2 about here]*

The twin sample used to generate the genetic clusters were taken from the Vietnam Twin Study of Aging (74, 90), and is described in detail in previous publications (4). A total of 1237 male-male twins participated in wave one of this longitudinal study, and a subset underwent MRI. The MRI study began in year 3 of the primary study. Only 6% of those invited to participate in the MRI study declined to do so. Others were excluded for the following reasons: possible metal in the body (7%); claustrophobia (3%); inability to travel to the test site (5%); exclusion of co-twin (9%); other reasons (3%). Scanning problems resulted in a loss of data for 8% of the participants. Included in the genetic analyses used to generate the clusters used in Chen et al. (4) and in the present paper were 406 middle-aged men, including 110 monozygotic and 93 dizygotic twin pairs. The mean age was 55.8 (±2.6) years (range: 51-59 years), and the mean level of education was 13.9 years (±2.1). The narrow age range is part of a design focusing on longitudinal age-related change within a narrowly defined cohort. Based on demographic and health characteristics, the sample is representative of US men in their age range (4, 90). Cortical variance in this sample is likely driven by several different factors, and previous studies have disentangled some of these, including testosterone (91, 92), cortisol (93) and cigarette smoking (94), as well as specific candidate genes, i.e. APOE (91) (95), in addition to general heritability (96).

**MRI data acquisition and analysis**

Imaging data (except VETSA data) were acquired using a 12-channel head coil on a 1.5-Tesla Siemens Avanto scanner (Siemens Medical Solutions, Erlangen, Germany) at Oslo University Hospital Rikshospitalet and St. Olav's University Hospital in Trondheim. The pulse sequences used for morphometric analysis were two repeated 3D T1-weighted magnetization prepared rapid gradient echo (MPRAGE), with the following parameters: Repetition time 2400 ms, echo time 3.61 ms, inversion time 1000 ms, flip angle 8°, matrix 192 × 192, field of view 192. Each volume consisted of 160 sagittal slices with voxel sizes 1.25 × 1.25 × 1.2 mm. Scanning time for each of these sequences was 7 min, 42 s. For the children between 4 and 9 years old in the MoBa-Neurocog sample, we used

a parallel imaging technique (iPAT), acquiring multiple T1 scans within a short scan time, enabling us to discard scans with residual movement and average the scans with sufficient quality. Previous studies have shown that accelerated imaging does not introduce significant measurement bias in surface-based measures when using FreeSurfer for image analysis, compared with a standard MPRAGE protocol with otherwise identical voxel dimensions and sequence parameters (97), which is in accordance with our own analyses. The protocol also included a 25-slices coronal T2-weighted fluid-attenuated inversion recovery sequence (TR/TE =7000–9000/109 ms) to aid the neuroradiological examination.

MRI data were processed and analyzed with FreeSurfer 5.3 (http://surfer.nmr.mgh.harvard.edu/) (71, 72) at the Neuroimaging Analysis Lab, Research Group for Lifespan Changes in Brain and Cognition, Department of Psychology, University of Oslo. This procedure yields a measure of cortical thickness for each person at each point on the reconstructed surface, and is capable of detecting sub-millimeter differences between groups (98-100). To extract reliable thickness estimates for each time point, images were automatically processed with the longitudinal stream (70) in FreeSurfer. Specifically an unbiased within-subject template space and image (69) is created using robust, inverse consistent registration (101). Several processing steps, such as skull stripping, Talairach transforms, atlas registration as well as spherical surface maps and parcellations are then initialized with common information from the within-subject template, significantly increasing reliability and statistical power (70). Maps were smoothed using a circularly symmetric Gaussian kernel with a full width at half maximum (FWHM) of 15 mm (102). FreeSurfer is an almost fully automated processing tool, and manual editing was not performed to avoid introducing errors. For the children, the issue of movement is especially important, as it could potentially induce bias in the analyses (73). All scans were manually rated for movement on a 1-4 scale, and only scans with ratings 1 and 2 (no visible or only very minor possible signs of movement) were included in the analyses, reducing the risk of movement affecting the results. Also, all reconstructed surfaces were inspected, and discarded if

they did not pass internal quality control. This led to the exclusion of 46 participants from MoBa-Neurocog and 9 from ND, reducing the total sample to the reported 1633 scans.

For VETSA, images were acquired on Siemens 1.5 Tesla scanners (241 participants at the University of California, San Diego; 233 participants at Massachusetts General Hospital). Sagittal T1-weighted MPRAGE sequences were employed with a TI=1000ms, TE=3.31ms, TR=2730ms, flip angle=7 degrees, slice thickness=1.33mm, voxel size 1.3x1.0x1.3mm.

*Cortical parcellation*

After surface reconstruction and thickness estimation, the cortex was parcellated in 12 separate genetic clusters of cortical thickness, each under maximal control of shared genetic influences. This was based on fuzzy cluster analyses of cortical thickness in an independent sample of 406 twins from the Vietnam Era Twin Study of Aging (VETSA) (74, 90), and the procedures and maps are described in detail elsewhere (4). In brief, cluster analyses were used to identify the boundaries of cortical divisions that were maximally genetically correlated (i.e., under control of shared genetic influences on cortical thickness).

**Statistical analyses**

First, all data from the entire age-span (4-89 years) were fitted to age by use of Generalized Additive Mixed Models (GAMM) implemented in R (www.r-project.org). GAMM was chosen because these models allow non-parametric fits with relaxed assumptions about the relationship between cortical thickness and age, with local smoothing effects, avoiding distant data points to affect the fit line in specific age ranges. GAMM allows flexible functional dependence of an outcome variable on covariates by using nonparametric regression, while accounting for correlations between observations by using random effects (103). Thus, using GAMM, we take advantage of both the longitudinal and cross-sectional information, and produce a non-parametric model fit in optimal

coherence with both. In contrast to polynomial models, the resulting estimated change trajectory is completely independent of any predefined model, allowing more realistic mapping of life-span trajectories of cortical change. These analyses included all 1633 observations. The GAMM fitting was run through the newly developed PING data portal (76), based on statistical processing using R (R Core Team)(104). Basically, this framework include regression analyses with automatic smoothness constrains (Wood, 2013, see Mixed GAM Computation Vehicle With GCV/AIC/REML Smoothness Estimation. Available online at: http://cran.r-project.org/web/packages/mgcv/index.html). We calculated Akaike Information Criterion (AIC) (77) and the Bayesian Information Criterion (BIC), which were used as measures of model fit to help guard against over-fitting.

Trajectories of cortical thickness from 4 to 89 years for mean thickness in the left and the right hemisphere were estimated. Close to identical fit lines were seen for left and right hemisphere, and the mean was therefore used for the rest of the analyses. As expected, sex had negligible effects on the age trajectories and on the absolute thickness measures (105), and was therefore not included as covariates in further analyses.

Next, linear mixed effect (LME) analyses as implemented in FreeSurfer (Bernal-Rusiel et al., NeuroImage 2013) were run to assess cortical thinning continuously across the surface in different age groups. This approach allows inclusion of participants with a single timepoint and to control for differences in inter-scan intervals. Participants with a single acquisition contributed to a more efficient and unbiased estimation of the between-participant variability. For these analyses, the intercept (mean) was considered as a random effect and the slope was taken as a fixed effect. The slope was calculated using the time between scans. Therefore, in this simple model, we considered parallel lines for different individuals. Although LME tools may allow evaluating different trajectories or more complex models, we could only use this model with a single random effect, because the

number of observations per participant was in most cases 2 and including more random effects would cause over-fitting of the data.

More specifically, for each group we used all the available scans to fit a LME where the intercept (mean) was considered as the single random effect and the time between scans (slope) was used as a fixed effect. For the youngest group, 'study' was included as an additional fixed effect since there were slight differences in scanning parameters. It should be noted that the model with a single random effect was the only possible model in our case, due to the fact that the majority of our participants had two acquisitions and the inclusion of more random effects would cause over-fitting of the data.

Therefore, the mathematical expression corresponding to this model were:

Considering the following variables:

$t_{ij}$ = time from baseline (in years)

$s_i$ = 1,2,3,4. Participant *i* belonging to a study sample (used only for the youngest group)

Then, the cortical thickness at each vertex was modeled as:

$$Y_i = \beta_1 + \beta_2\, t_{ij} + \beta_3\, s_i + e_{ij}$$

Where $b_1$ is the weight corresponding to the random effect for the mean (or intercept) and $\beta_{1,2,3}$ are the beta weights corresponding to the mean, the time between scans and the study respectively. Finally, $e_{ij}$ is the measurement error for each participant at each timepoint.

After model estimation (i.e., determination of model parameters and coefficients using optimization procedures), we tested the effect of time by doing F tests on the time variable. The vertex-wise results of the F-tests indicated the thinning/thickening of the cortex according to scanning time.

Mean participant-specific thickness (intercept) and the effect of the study were regressed out by introducing them as covariates in the test.

Additionally, we estimated symmetrized annual percent change (APC) continuously across the surface using only longitudinal data. Maps of APC were created by a use of a surface-based smoothing spline approach implemented in Matlab, where a nonparametric local smoothing model, the smoothing spline, was fitted to the data (78).

For the genetic clustering analyses, GAMM was first used to estimate the trajectories of cortical thickness change throughout the age-span of the study in each of the 12 clusters, and plotted against the mean of all. To be able to compare the structure of cortical development and aging to the genetic patterning of thickness, thickness change in each cluster was correlated pairwise with change in all other clusters, with mean change regressed out, and the resulting correlation matrices presented as a heat map. This was compared to the correlation map of the genetic correlations between each of the 12 clusters by use of the Mantel test (79), implemented in R, with 9999 replications. The Mantel test is a permutation procedure that yields a measure of the correlation between two matrices. These analyses were run separately for the young part of the sample (age < 20 years) and the adult part of the sample (age $\geq$ 20 years), to disentangling possible differences in how the genetic pattern was related to the pattern of change due to childhood development vs. change due to adult ”aging”. These analyses were restricted to the participants with two or more time points, and so were exclusively longitudinal. To identify clusters of correlations that could be compared across matrices, the community structure or modules in the change (developmental and aging) and genetic correlations matrices were obtained using the Louvain algorithm (80), part of the Brain Connectivity Toolbox (http://www.brain-connectivity-toolbox.net, (81). The optimal community structure is a subdivision of the network into non-overlapping groups of regions in a way that maximizes within-group connection strength, and minimizes between-group strength. The community structure may

vary from run to run due to heuristics in the algorithm, so 10 000 iterations of the algorithm were run, and each region assigned to the module it was most often associated with (by taking the mode of the module assignment across iterations).

**Replication analyses after strict birth weight and intellectual ability exclusion criteria**

GAMM fitting were run separately for the full MoBa-Neurocog sample (age $\leq$ 12 years) and the MoBa-Neurocog sample restricted to those with birth weight between 2500g and 4500g and scoring at least 1 SD above the population mean on WPSSI or WASI. The results showed indistinguishable trajectories of cortical thickness, demonstrating that the reported results were not due to low-functioning parts of the sample. Results for left and right hemisphere mean cortical thickness are shown in Supplemental Figure 2.

*[Insert Supplemental Figure 2 about here]*

**Aging community structure and replication analyses**

Applying the Louvain algorithm to the adult change data and organizing the relationships between clusters according to this algorithm yielded the matrix in Supplemental Figure 3.

*[Insert Supplemental Figure 3 about here]*

The values are identical to those in the right panel in Figure 3, but the order of the clusters is different. Cluster-order: 1,3,4,2,7, 10,11,8,12,9,6,5. The first and the third group of clusters are identical to two groups found in development and the genetic organization, while the remaining two development/ genetic organizations are compiled into one big group in aging.

We also re-ran this analysis for the participants above 50 years, and the results were very similar (20 year and up to the left, 50 years and up to the right), with the Mantel test yielding $r^2 = .99$, $p < 10e^{-5}$ when compared to the structure of the genetic clusters.

*[Insert Supplemental Figure 4 about here]*

Analyses were also run without APC regressed out, which did not influence the observed correlation pattern much, and the Mantel test showed that the matrices both for development and adult changes still were similar to the genetic matrix (both p's $< 10e^{-5}$). With APC regressed out, however, the figures are easier to interpret visually since correlations are then both positive and negative, using the whole heat-map scale, instead of only showing differences in positive relationships. The genetic clusters used in the present paper were derived from VETSA data adjusted for average cortical thickness, to allow examination of region-specific genetic effects (4).

**Supplemental Figure legends**

**Supplemental Figure 1 Number of participants across the age-span**

**Supplemental Figure 2 Replication of results in normal birth weight children**

GAMM fitting were run separately for the full MoBa-Neurocog sample (age $\leq$ 12 years) and the MoBa-Neurocog sample restricted to those with birth weight between 2500g and 4500g and scoring at least 1 SD above the population mean on WPSSI or WASI.

**Supplemental Figure 3** Applying the Louvain algorithm to the adult change data

The values are identical to those in the right panel in Figure 3, but the order of the clusters is 1,3,4,2,7, 10,11,8,12,9,6,5. The first and the third group of clusters are identical to two groups found in development and the genetic organization, while the remaining two development/ genetic organizations are compiled into one big group in aging.

**Supplemental Figure 4 Correlation pattern in aging vs. whole adult age span**

We also re-ran the cluster-correlation analyses for the participants above 50 years, and the results were very similar (20 year and up to the left, 50 years and up to the right).